

Confocal microscopy of thick specimens

S. Nadar S. Reihani^{a,b} and Lene B. Oddershede^{b,*}

^aInstitute for Advanced Studies in Basic Sciences (IASBS), P.O. Box 45195-1159, Zanjan, Iran

^bNiels Bohr Institute, Blegdamsvej 17, 2100 Copenhagen Ø, Denmark

Abstract. Confocal microscopy is an excellent tool to gain structural information from deep within a biological sample. The depth from which information can be extracted as well as the resolution of the detection system are limited by spherical aberrations in the laser pathway. These spherical aberrations of the visible light can be efficiently canceled by optimizing the refractive index of the immersion media. Another way of canceling spherical aberrations is by changing tube length, or alternatively, by changing the objective from infinite correction to finite correction, or vice versa, depending on which microscope is used. A combination of these two methods allows for confocal imaging at continuous depths. Presently, confocal microscopes typically operate at a maximum depth of 40 μm in the sample, but with the methods presented here, we show that information can easily be gained from depths up to 100 μm . Additionally, the precision of localization of a single fluorophore in the axial direction, limited by spherical aberrations, can be significantly improved, even if the fluorophore is located deep within the sample. In principle, this method can improve the efficiency of any kind of microscopy based on visible light. © 2009 Society of Photo-Optical Instrumentation Engineers. [DOI: 10.1117/1.3156813]

Keywords: confocal microscopy; spherical aberrations; resolution; fluorescence; bioimaging.

Paper 09040LR received Feb. 9, 2009; revised manuscript received Mar. 26, 2009; accepted for publication Apr. 7, 2009; published online Jun. 29, 2009.

The resolution and signal level of confocal microscopy dramatically drops as the focus depth is increased due to the spherical aberrations (SA) induced by refractive index mismatch between immersion and specimen. At a depth of 5 μm the signal level falls to 40% of the value just above the coverslip; in a depth of 15 μm only 10% is left.¹ Therefore, in order to gain information from deep within a sample, it is necessary to compensate SA. Different static methods such as alteration of the tube length,² introducing an iris to decrease the pupil area of the objective,³ and dynamic methods such as deformable mirrors⁴ are proposed to compensate the SA. These methods are rather expensive, hard to implement, or need intensive computation. Not only resolution of confocal microscopy but also, e.g., the precision of localization of individual fluorophores in the axial direction is limited by SA.⁵ The simple method presented here can improve confocal microscopy such that information can easily be gained from depths of 100 μm , a resolution comparable to two-photon microscopy.⁶

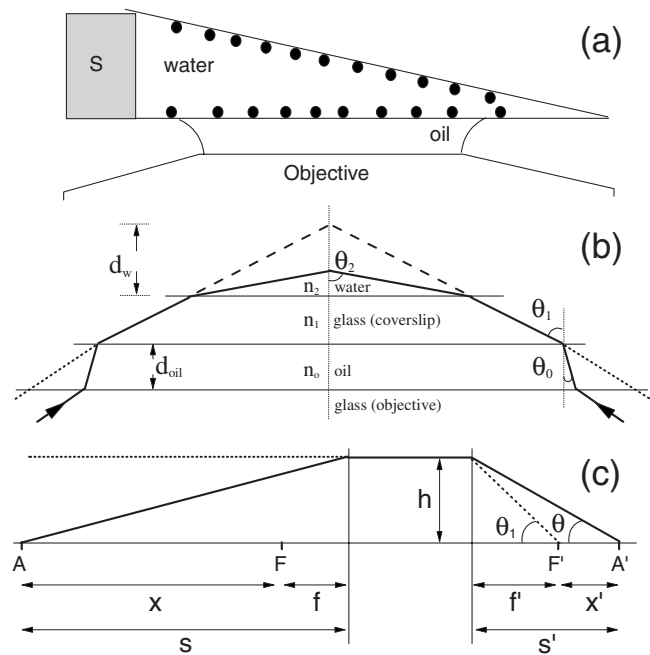


Fig. 1 Schematic drawings of: (a) Sample chamber, where a spacer (S) is used to make a chamber with gold nanoparticles (●) at different depths. (b) Optical path of the marginal rays when the glasses and the immersion medium are index matched (dotted line) and mismatched (solid line). The dashed line shows the nominal focus. (c) The effect of changing tube length.

The SA appear as a phase in the intensity point spread function⁷:

$$\Psi_{\text{total}} = \Psi_{\text{tube}} + \Psi_{\text{obj}} + \Psi_{\text{im/cg}} + \Psi_{\text{cg/s}}, \quad (1)$$

where Ψ_{tube} stems from the tube length, Ψ_{obj} stems from the objective, and $\Psi_{\text{im/cg}}$ and $\Psi_{\text{cg/s}}$ denote the SA introduced by the possible mismatch in refractive indices of the coverglass and the immersion media of the objective and of the media within the sample, respectively. Minimizing Ψ_{total} at any given depth produces the most focused laser beam, the optimal signal, and the best resolution. The idea presented here is to modify both the first, Ψ_{tube} , and third, $\Psi_{\text{im/cg}}$, terms of the right-hand side of Eq. (1), such that they optimally cancel the phases introduced by the other terms. The two modifications have been individually reported to have an influence on the stability of an optical trap based on infrared light.⁸⁻¹⁰

The experiment was performed using a scanning confocal microscope (Leica SP5) with an infinity tube length corrected (ITLC) objective (Leica HCX PL Apo, 63x, NA = 1.32, ∞ , 0.17) or a finite tube length corrected (FTLC) objective (Leitz, PL APO, 100x, NA = 1.32, 170, 0.17). Figure 1 shows a schematic drawing of the sample chamber. Two cover glasses (Menzel Glaser, #1.5) were separated at one side by means of two stripes of double-stick tape to have gold nanoparticles attached to the cover glasses at various heights inside the chamber [Fig. 1(a)]. The diameter of the gold nanoparticles was 80 nm (BBInternational). The size was chosen so that they would provide a reasonable signal level in the non-aberrated case. The inner surface of the lower coverslip was

*Address all correspondence to: L. B. Oddershede, E-mail: oddershede@nbi.dk

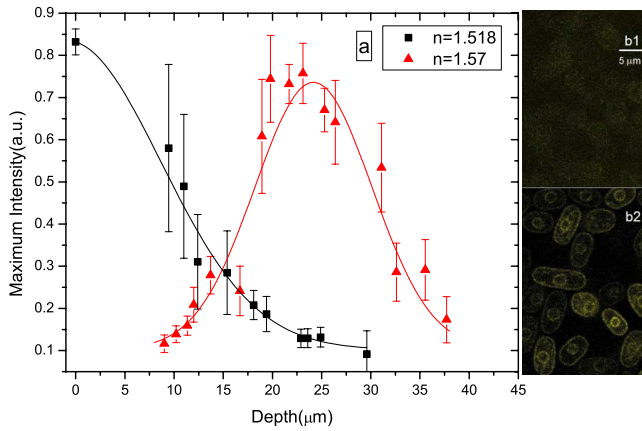


Fig. 2 (a) The maximum signal intensity for confocal visualization of 80-nm gold nanoparticles at different depths using an ITLC objective and two different immersion media. The right side shows fluorescent images of *S. pombe* yeast cells at a depth of 8 μm using two different immersion media: in b1 $n=1.518$; in b2 $n=1.538$.

chosen as zero for the depth measurements. The depth of the gold nanoparticles attached to the upper coverslip was measured as the distance traveled by the objective until the particular particle was in focus. To visualize the gold nanoparticles, we used immersion oils used with different refractive indices from Cargille (refractive index liquids set A). After deducting the average background intensity from all pixels, the maximum intensities at the positions of the nanoparticles were measured and the difference between the maximum intensity and the background noise at a given depth can be used as a measure of the confocal visualization efficiency. The gold beads were visualized by the reflection of a 488-nm laser line

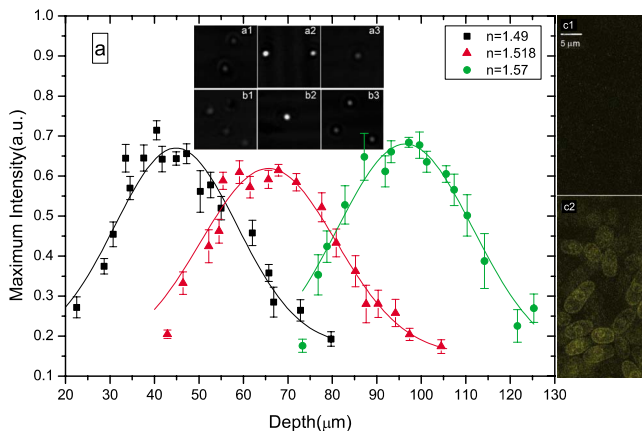


Fig. 3 (a) Maximum intensity level for confocal visualization of 80-nm gold nanoparticles as a function of depth for different immersion media. An FTLC objective was used in a microscope designed for an ITLC objective. The inset shows two rows of corresponding confocal images (each $3.85 \times 3.85 \mu\text{m}^2$) at various depths using two different immersion oils. Upper row: $n=1.518$ and the imaging depths are 42.9, 65.5, and 104.5 μm , respectively. Lower row: $n=1.57$ and the imaging depths are 73.3, 93.3, and 121.6 μm , respectively. The right side shows confocal images of fluorescent *S. pombe* yeast cells at a depth of $\sim 40 \mu\text{m}$ using normal immersion oil ($n=1.518$) and the ITLC objective (c1) or the FTLC objective (c2).

(operated at 43% of maximum power) with the following settings: zoom 65, pinhole 600 μm , and field of view $3.84 \times 3.84 \mu\text{m}^2$.

Also, we tested the method on a sample containing a dense solution of living *Schizosaccharomyces pombe* yeast cells. The *S. pombe* yeast cells expressed green fluorescent protein (GFP) in all membrane parts and were visualized by exciting the GFP by a 514-nm laser line (using 92% of maximum power). The following settings were used: zoom 3.7, pinhole 152 μm , and field of view $42 \times 42 \mu\text{m}^2$. The “set A” immersion oils used for visualizing the gold nanoparticles had autofluorescence in the same interval as GFP emission. Therefore, we used either the standard Leica immersion oil ($n=1.518$) or a nonfluorescent custom-made Cargille immersion oil ($n=1.538$, code 1160, lot 071884) for confocal visualization of the fluorescent yeast cells.

The SA due to the refractive index mismatch at a depth of d_w in the second medium can be written as²

$$\Psi_{\text{cg/s}}(\theta_1, \theta_2, -d_w) = -k_0 d_w (n_1 \cos \theta_1 - n_2 \cos \theta_2), \quad (2)$$

where θ_1 , θ_2 , k_0 , and d_w are the incident angle in first medium, refracted angle in second medium, wave number in vacuum, and nominal depth of focus, i.e., the distance traveled by the objective, respectively, and n_1 and n_2 are the refractive indices of the first and the second media [see Fig. 1(b)]. Hence, one way to increase the depth at which SA are minimized, d_w , is to change index of refraction of the immersion media.⁸

If one wishes to image significantly deeper into the sample than can be done by just changing the refractive index of the immersion media, the tube length can be changed.⁹ Changing tube length in a commercial confocal microscope would be very cumbersome. Therefore, we performed another optical change that in effect corresponds to changing the tube length. If the microscope is designed to have parallel light entering the objective, one should use an ITLC objective for optimal visualization. If, instead, one uses an FTLC objective in a such a microscope, this corresponds to changing the tube length. Figure 1(c) shows the change in optical path of marginal rays corresponding to changing the objective from ITLC to FTLC. Consider a perfect lens, of some thickness, designed to image an axial point-like object A' to A [full line in Fig. 1(c)]. The phase introduced by the lens for the marginal ray (with respect to the axial ray) that crosses the lens a distance h above the optical axis can be written as²:

$$\Psi_{\text{finite}} = k_0 [S - \sqrt{S^2 + h^2} + n(S' - \sqrt{S'^2 + h^2})] \quad (3)$$

where the distances S , S' , and h are as defined in Fig. 1(c), and n is the index of refraction of the immersion media. Likewise, the distances f , f' , X , and X' are defined in Figure 1(c). Knowing the NA, the tube length (X), the magnification (M) of the objective, and considering the relations $f=X/M$, $f'=nf$, $X'=f'/M$, $S=X+f$, and $S'=X'+f'$, all unknown parameters of Eq. (3) except h can be found. In the present experiments $X=170 \text{ mm}$, $M=100$, and $\text{NA}=1.32$. Hence, the above parameters become $f=1.7 \text{ mm}$, $f'=2.58 \text{ mm}$, and $X'=25.8 \mu\text{m}$, respectively. The only remaining unknown, h , can be calculated as $h=S' \tan \theta$ [see Fig. 1(c)] with $\theta = \arcsin(\text{NA}/n)$ and $n=1.518$, giving $h=2.6 \text{ mm}$. Substituting these values in Eq. (3) results in $\psi_{170} = -4.05k_0$. If, on the

other hand, an ITLC objective is used [dotted line in Fig. 1(c)] one can rewrite Eq. (3) as $\Psi_{\infty} = k_0[n(f' - \sqrt{f'^2 + h^2})]$. Inserting values for f' and h we get $\psi_{\infty} = -4.01k_0$. Therefore, the phase induced by changing the tube length from 170 mm to infinity will be $\Psi_{\text{tube}} = \psi_{\infty} - \psi_{170} = 0.04k_0$.

The term $\Psi_{\text{cg/s}}$ from Eq. (2) gives the contribution from the sample to the SA induced. Assuming that h remains constant, $\theta_1 = \arctan(h/f') = 60.7$ deg. Substituting this value along with $n_1 = 1.518$ and $n_2 = 1.33$ in Eq. (2) results in $\Psi_{\text{cg/s}} = -0.58k_0d_w$. In the case where the coverglass and the immersion medium are index matched ($n = 1.518$), $\Psi_{\text{imm/cg}}$ in Eq. (1) vanishes, hence, the optimal microscopy depth is at the point where $\Psi_{\text{total}} = \Delta\Psi_{\text{tube}} + \Psi_{\text{cg/s}} = 0$, which corresponds to $d_{w,\text{tube}} = 69 \mu\text{m}$. In other words, using the FTLC objective in a microscope designed for an ITLC objective causes the optimal confocal visualization depth to be $69 \mu\text{m}$.

To have a continuous change of imaging depth a change of objective can be combined with a change of refractive index of the immersion media. Following the argumentation of Ref. 8, an increase of refractive index of the immersion medium by $\Delta n = 0.01$ implies $\theta_0 = 60.0$ deg (note that $\theta_1 = 60.7$ deg). Thus, the component of the phase factor arising from the oil-glass interface can be written as $\Psi_{\text{imm/cg}} = 0.021k_0d_o$. The thickness of the immersion oil layer, d_o , was measured for the FTLC objective to be $210 \pm 9 \mu\text{m}$. Balancing the second and the third terms of Eq. (1) ($\Psi_{\text{imm/cg}} + \Psi_{\text{cg/s}} = 0$) results in $d_w = 7.6 \pm 0.3 \mu\text{m}$. Hence, if an FTLC objective is used instead of an ITLC objective in a microscope designed for an ITLC objective, an increase of $\Delta n = 0.01$ will increase the optimal microscopy depth, d_w , by $7.6 \pm 0.3 \mu\text{m}$.

To experimentally test how confocal visualization depends on the refractive index of the immersion oil, 80-nm gold particles at different depths were imaged using an ITLC objective with two different immersion media. Each data point in Fig. 2(a) is an average of at least 10 measurements and the error bars show the standard deviation. Figure 2(a) illustrates that: (1) The maximum intensity for the normal immersion oil ($n = 1.518$) occurs at the glass surface or zero depth. (2) Increasing the refractive index of the immersion media shifts the optimum microscopy depth, as measured by the maximum intensity of the gold nanoparticles, deeper into the sample chamber. Hence, by changing the index of refraction of the immersion media, one can easily shift the optimal imaging depth by 20 to 30 μm . (3) A shift in the immersion media index of refraction from $n = 1.518$ to $n = 1.57$ causes a shift in optimal microscopy depth of $24.1 \pm 0.2 \mu\text{m}$. This shift is in excellent agreement with the predicted value of $\Delta d_w = 4.1 \pm 0.5 \mu\text{m}$ per $\Delta n = 0.01$.⁸ (4) The FWHM (full width at half maximum) of the graph is $\sim 16 \mu\text{m}$. This implies that if a particular immersion oil is chosen, then the confocal visualization is very efficient within an axial distance of $\sim 16 \mu\text{m}$. The right side of Fig. 2 shows confocal images of GFP expressing *S. pombe* yeast cells 8 μm from the surface using the normal immersion oil (b1) or the improved method (b2).

Finally, the combination of using an FTLC objective with changing refractive index of the immersion oil was experimentally tested. The inset of Fig. 3 shows confocal images of gold nanoparticles in a setup where an FTLC objective was used in a microscope designed for ITLC objectives. Each row

of pictures is taken with a different immersion oil, and the depth increases throughout each row. Noticeable is the fact that the sharpest picture of experiments with $n = 1.49, 1.518,$ and 1.57 appear for depths of 45, 65, and 96 μm , respectively. The larger the index of refraction, the deeper into the sample is the most efficient confocal visualization. Figure 3(a) illustrates that: (1) Increasing the refractive index of the immersion medium shifts the optimal microscopy deeper into the sample. Efficient confocal visualization is even possible as deep as 100 μm into the sample. (2) The graphs have FWHMs of $\sim 40 \mu\text{m}$, which is more than twice that of the situation depicted in Fig. 2. (3) The immersion oil recommended by the manufacturer with $n = 1.518$ provides an optimal visualization at a depth of $\sim 65 \mu\text{m}$, which is in good agreement with our estimated value of 69 μm . (4) A 0.01 change in n of the immersion media provides an ~ 6 - to 7- μm shift in the optimal microscopy depth, in agreement with the theoretically estimated value of $7.6 \pm 0.3 \mu\text{m}$. The right part of Fig. 3 illustrates the effect of using an FTLC objective in a microscope designed for ITLC objectives for a dense biological sample of fluorescently marked *S. pombe* yeast cells: There is no visible signal at a depth of 40 μm if the ITLC objective is used (c1), but a good signal-to-noise ratio results with the FTLC objective (c2).

We presented a simple, easily implementable, and low-cost method to significantly improve confocal microscopy by canceling spherical aberrations. The spherical aberrations can be canceled by changing immersion media, possibly in combination with changing the objective from infinite correction to finite correction. We have shown efficient confocal visualization at any depth up to 100 μm inside the sample, depths which are comparable to those reachable by two-photon microscopy. In principle, any microscopy based on visible light, including two-photon microscopy, can be similarly improved by this method.

References

1. J. B. Pawley, Ed., *Handbook of Biological Confocal Microscopy*, 3rd ed., Springer, New York (2006).
2. C. J. R. Sheppard and M. Gu, "Aberration compensation in confocal microscopy," *Appl. Opt.* **30**, 3563–3568 (1991).
3. M. J. Booth and T. Wilson, "Strategies for the compensation of specimen-induced spherical aberration in confocal microscopy of skin," *J. Microsc.* **200**, 68–74 (2000).
4. L. Sherman, J. Y. Ye, O. Albert, and T. B. Norris, "Adaptive correction of depth induced aberrations in multiphoton confocal microscopy using a deformable mirror," *J. Microsc.* **206**, 65–71 (2001).
5. B. Huang, S. A. Jones, B. Brandenburg, and X. Zhuang, "Whole-cell 3D STORM reveals interactions between cellular structures with nanometer-scale resolution," *Nat. Methods* **5**, 1047–1052 (2008).
6. H. C. Gerritsen and C. J. de Grauw, "Imaging of optically thick specimen using two-photon excitation microscopy," *Microsc. Res. Tech.* **47**, 206–209 (1999).
7. P. C. Ke and M. Gu, "Characterization of trapping force in the presence of spherical aberration," *J. Mod. Opt.* **45**, 2159–2168 (1998).
8. S. N. S. Reihani and L. B. Oddershede, "Optimizing immersion media refractive index improves optical trapping by compensating spherical aberrations," *Opt. Lett.* **32**, 1998–2000 (2007).
9. S. N. S. Reihani, M. A. Charsooghi, H. R. Kholesifard, and R. Golestanian, "Efficient in-depth trapping with an oil-immersion objective lens," *Opt. Lett.* **31**, 766–768 (2006).
10. S. N. S. Reihani, H. R. Kholesifard, and R. Golestanian, "Measuring lateral efficiency of the trap: the effect of tube length," *Opt. Commun.* **259**, 204–211 (2006).